Preparation and photophysical studies of [Ln(hfac)3DPEPO], Ln = Eu, Tb, Yb, Nd, Gd; interpretation of total photoluminescence quantum yields

Post-print of a peer-reviewed article published by the Royal Society of Chemistry.
Published article available at: http://dx.doi.org/10.1039/C3DT51380G

Cite as:
Congiu, M., Alamiry, M., Moudam, O., Ciorba, S., Richardson, P. R., Maron, L., Jones, A. C., Richards, B. S., & Robertson, N. (2013). Preparation and photophysical studies of [Ln(hfac)$_3$DPEPO], Ln = Eu, Tb, Yb, Nd, Gd; interpretation of total photoluminescence quantum yields. *Dalton Transactions*, 42(37), 13537-45.

Manuscript received: 27/05/2013; Accepted: 19/07/2013; Article published: 30/07/2013

Preparation and photophysical studies of [Ln(hfac)$_3$DPEPO], Ln= Eu, Tb, Yb, Nd, Gd; interpretation of total photoluminescence quantum yields**†

Martina Congiu,[1] Mohamed Alamiry,[1] Omar Moudam,[1] Serena Ciorba,[2] Patricia R. Richardson,[1] Laurent Maron,[3] Anita C. Jones,[1] Bryce S. Richards[2] and Neil Robertson[1,*]

[1]EaStCHEM, School of Chemistry, Joseph Black Building, University of Edinburgh, West Mains Road, Edinburgh, EH9 3JJ, UK.

[2]School of Engineering and Physical Science, Heriot-Watt University, Edinburgh, UK.

[3]Laboratoire de Physique et Chimie de Nano-objets, Institut National des Sciences Appliquées, 135 avenue de Rangueil, Toulouse, Cedex 4, France.

[*]Corresponding author; e-mail: neil.robertson@ed.ac.uk

[**]We thank Regione Autonoma della Sardegna for a scholarship (MC) and the EPSRC for funding. LM is a member of the Institut Universitaire de France and also would like to thank the Humboldt foundation for a grant of experienced researcher. LM is also grateful to CINES and CalMip for a generous grant of computing time. We thanks Anna Collins for the structural data collection and solution.

[†]Celebrating 300 years of Chemistry at Edinburgh.

Supporting information:
[‡]Electronic supplementary information (ESI) available: Figure S1–S6: NMR spectra of [Ln(hfac)$_3$DPEPO] complexes; Figure S7: asymmetric unit of [Gd(hfac)$_3$DPEPO]; Figure S8: optimised structures of the ground state and of the lowest energy triplet spin state of [Eu(hfac)$_3$(DPEPO)]; Figure S9: emission and excitation spectra of [Tb(hfac)$_3$DPEPO]; Table S1: selected bond lengths and angles for [Gd(hfac)$_3$DPEPO]; Table S2: selected calculated bond-lengths and angles for [Eu(hfac)$_3$DPEPO] in the lowest singlet state; Table S3: selected calculated bond-lengths and angles for [Eu(hfac)$_3$DPEPO] in the lowest triplet state. CCDC 941149. For ESI and crystallographic data in CIF or other electronic format see http://dx.doi.org/10.1039/C3DT51380G

Abstract

Synthesis and photophysical characterisation of [Ln(hfac)$_3$DPEPO] complexes (with Ln= Eu, Tb, Yb, Nd, Gd) has been carried out to investigate the factors responsible for the variation in total photoluminescence quantum yield within this family of emissive lanthanide complexes. Electronic absorption and emission spectroscopy, in conjunction with DFT calculations of the excited state of the Eu complex, elucidate the role of each ligand in the sensitisation of the lanthanide through the antenna effect. The X-ray crystal structure of [Gd(hfac)$_3$DPEPO] has been determined and shows an 8-coordinate environment around the Gd and a ten-membered chelate ring involving the DPEPO ligand. Total photoluminescence quantum yields were measured to be 6%, 1% and 2% for Ln = Tb, Nd and Yb, respectively, in comparison with around 80% for Ln = Eu. The lower quantum yield for Nd and Yb, compared with Eu, can be attributed to more efficient quenching of the excited Ln state by high-energy oscillations within the ligands, whereas the lower quantum yield for Tb is assigned to a combination of poor energy transfer from the ligand excited state to the Tb and longer radiative lifetime.

Introduction

Lanthanide chemistry has seen widespread use in different fields, such as biochemical studies,[1, 2] therapeutical applications,[3] as well as photonic and electronic materials,[2, 4-6] promoted by attractive photophysical properties: long-lived excited states and narrow band emission.[7-11] Energy levels within each lanthanide ion are determined according to their $4f^n$ electronic configuration. These energies are predominantly determined by interelectronic repulsion and spin-orbit coupling, with ligand field effects playing a negligible role. Electric dipole transitions between f-f states are parity forbidden and lanthanide complexes have low absorption coefficients ($\varepsilon < 10$ M^{-1} cm^{-1}) and radiative lifetimes on the millisecond time scale.

By introducing an appropriate chromophore (usually referred to as an "antenna") it is possible to increase the complex's absorbance in the visible and UV regions.[8, 12] The antenna effect is an energy conversion process which involves a ligand able to collect the light and an emitting lanthanide ion. Usually such ligands are highly π-conjugated systems, aromatic or hetero-aromatic, with high molar absorption coefficients. Once the ligand singlet-excited state has been reached, it may typically convert to a triplet state by intersystem crossing (facilitated by the presence of the heavy lanthanide ion). The triplet energy level needs to be sufficiently above the emissive lanthanide state for the latter to accept efficiently the energy from the chromophore. Excitation of the coordinated metal centre is then possible by way of energy transfer from the triplet state of the ligand. The overall efficiency of this photoluminescence process depends on different factors; the absorption coefficient of the ligand, the efficiency of the ligand-to-metal energy transfer and the efficiency of the metal luminescence.[12]

The unique properties of lanthanides have attracted attention within the area of solar energy conversion. The first application in light-concentration devices was in the 1970s,[13, 14] when Weber and Goetzberger included lanthanide-based materials in fluorescent collectors, to trap incoming light through a wide plane surface and transfer it via total internal reflection to Si solar cells at the edge of the collector. Recent studies on such luminescent solar concentrators (LSCs) using lanthanides have focused on extending the absorption wavelength of the compounds[15] in order to take advantage of the inherently low self-absorption and maximise the high geometric gain.[16] Solar energy utilisation may also be enhanced through luminescent down-shifting (LDS), in which the luminescent material absorbs at short wavelength and re-emits at a longer one where the solar cell more strongly absorbs.[17, 18]

The use of β-diketonates as ligands can effectively tune the harvesting of light as well as allowing ligand-to-metal energy transfer. Excitation at around 300 nm,[19] due to the intense π-π* transition, has made β-diketonates an important class of antenna.[8] Previously,[20-24] the synthesis of lanthanide complexes with β-diketonate and phosphine oxide ligands has been studied, because of the ability of phosphine oxide ligands to prevent coordination of solvent molecules and also their intrinsic low-frequency vibrations, due to the presence of P=O, minimise radiationless quenching of the Ln excited state. In this context, we previously reported the complex [Eu(hfac)$_3$DPEPO][25], where DPEPO = bis(2-(diphenylphosphino)phenyl)ether oxide, and hfac = hexafluoroacetylacetonate. This complex was found to have an unprecedentedly high value of PLQY in polymethylmethacrylate (PMMA) of 80%,[25] and we subsequently studied the complex in luminescent materials for solar energy conversion.[11,18] The DPEPO ligand, previously used by Xu *et al.* [23], shows good coordination ability and confers rigidity to the complex. In this work, to fully probe the origins of this exceptional PLQY and aid the further development of such complexes, we extend the study to analogues of [Eu(hfac)$_3$DPEPO], using Tb^{3+}, Nd^{3+}, Yb^{3+} and Gd^{3+}, focusing on the role of the different ligands in the energy transfer process, the luminescence efficiency of the lanthanide centres and the resulting total PLQY. Tb^{3+}, like Eu^{3+}, is a technologically-important visible emitter; Yb^{3+} and Nd^{3+} enable the study to be extended to near-IR emitters; and Gd^{3+} enables specific insights into the excited ligand energy levels.

Results and discussion

The new series of complexes has the general formula [Ln(hfac)$_3$DPEPO], with Ln = Tb^{3+}, Nd^{3+}, Yb^{3+}, Gd^{3+} and hfac = hexafluoroacetylacetonate anion (Figure 1). All the molecules have been fully characterised by ^{1}H-NMR, elemental analysis, mass spectrometry, UV/Vis, steady-state and time-resolved emission spectroscopy, and quantum yield determination. DFT calculations were performed on the Eu complex, which, together with determination of the [Gd(hfac)$_3$DPEPO] X-ray crystal structure, gave additional insight into the photophysical processes.

All the complexes were analysed by ^{1}H-NMR in *d*-chloroform solution. Although the peaks in the spectra

were broadened by the paramagnetism of the lanthanide ions, there were similarities with previous complexes reported using the DPEPO ligand.[23] When the DPEPO is complexed with the lanthanide, a signal shift is observed due to the deshielding effect of the paramagnetic lanthanide ion. The mixed peaks of the phenyl groups are shifted to high frequency and the proton of the hfac group appears in the range 5 - 6 ppm (Fig S1 – S6†).

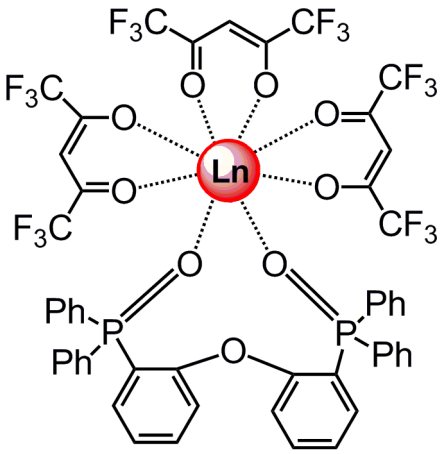

Figure 1. General molecular structure of [Ln(hfac)$_3$(DPEPO)]: Ln = Eu, Tb, Yb, Nd and Gd.

A crystal structure was obtained for [Gd(hfac)$_3$DPEPO]. The system crystallised with two molecules in the asymmetric unit with the expected eight-coordinate environment of the Gd(III) centre, which excludes other ligands such as H_2O which, for the Eu, Tb, Nd and Yb complexes, might increase non-radiative decay of the excited state through coupling with high-energy O-H oscillators. For clarity, only one molecule of [Gd(hfac)$_3$(DPEPO)] is shown (Figure 2, 3) (with the full unit cell containing Gd(1) and Gd(101)) shown in ESI (Fig S7†)). The general coordination environment of each Gd centre is similar and is described below for Gd(1).

Gd(1) is coordinated to two oxygen atoms, O(1) and O(2), of the DPEPO ligand and its coordination sphere is completed by the other six oxygen atoms belonging to the three hfac ligands. It is notable that the ether oxygen of the DPEPO ligand, O(3), does not coordinate the Gd, as the distance between these two atoms Gd(1)-O(3) is too large (3.686 Å). This leads to a very unusual ten-membered chelate ring, which is a rare situation in terms of the chelate effect on complex stability.[26, 27] Despite the widespread interest in Ln complexes with β-diketonate and phosphine oxide ligands, there are no other structurally-determined species of similar structure in the literature.[28] Analogous structures of Gd with hfac ligands include a [Gd(hfac)$_3$(H_2O)$_2$] unit, from crystals of [Re(CO)$_3$Cl(dpq)][Gd(hfac)$_3$(H_2O)$_2$]•C_6H_6,[29] and structures of formula [Gd(hfac)$_3$(nitronylnitroxide)].[30] These structures show Gd ion coordination geometry with hfac in

general agreement with that of [Gd(hfac)$_3$(DPEPO)] (Table S1). The average Gd···O bond length in [Gd(hfac)$_3$(DPEPO)] is 2.403 Å, similar to the average bond for the Gd-hfac unit (2.364 Å) shown by Kennedy *et al*.[29] This value can be compared to Eu analogues in which the average bond length for β-diketonate complexes show values of 2.395 Å ([Eu(hfac)$_3$(bpyO$_2$)]·0.5C$_6$H$_6$[31]) to 2.430 Å (Eu(hfac)$_3$(dmbipy)(H$_2$O)[32]). Since the 4f electrons of the metal are shielded by 5p^6 and 6s^2 electrons, they are not readily available for covalent bonds with the ligands. Hence electrostatic interactions mostly determine the geometry of the molecule, alongside any steric factors arising from the ligand itself. For this reason, lanthanide complexes with the same ligands are often isostructural, although the size of the central ion steadily decreases across the series and differences may occur between the early and the late lanthanide ions. As adjacent elements, the metallic radii of Gd(III) and Eu(III) are very similar and this gives confidence in using structural and photophysical data from [Gd(hfac)$_3$(DPEPO)] in the interpretation of [Eu(hfac)$_3$(DPEPO)] and its analogues.

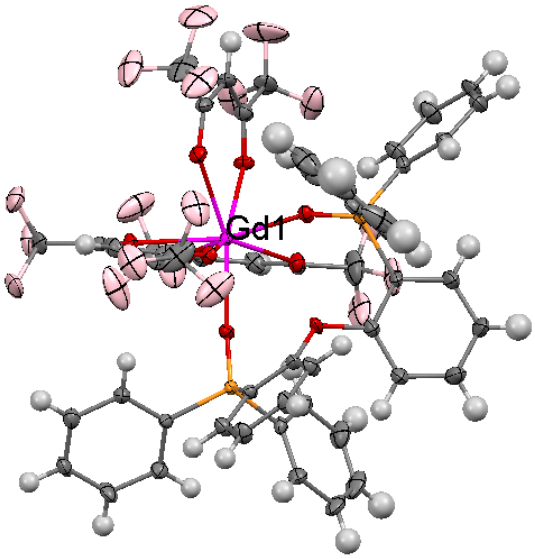

Figure 2. X-ray structure of [Gd(hfac)$_3$(DPEPO)] with thermal ellipsoids set at 30%.

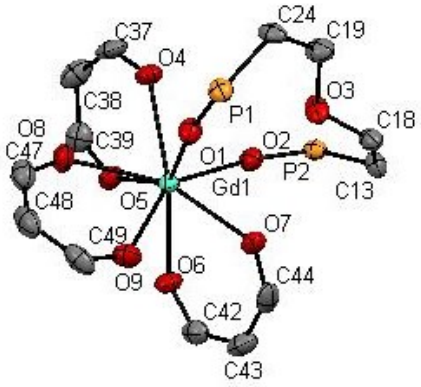

Figure 3. The structure of [Gd(hfac)$_3$(DPEPO)] with thermal ellipsoids at 30%. H and F atoms and phenyl groups have been removed to illustrate the coordination environment of the Gd.

Comparing the $[Gd(hfac)_3(H_2O)_2]$[29] structure with $[Gd(hfac)_3DPEPO]$ highlights the influence of the bulky DPEPO ligand on the molecule. In $[Gd(hfac)_3(H_2O)_2]$, the Gd atom is eight-coordinate, forming two planes, created, in one case, by two hfac ligands and the other by two molecules of water and the other hfac.[29] In contrast, for $[Gd(hfac)_3DPEPO]$ the introduction of the DPEPO ligand compresses the hfac ligands and forces them to a different spatial arrangement. The angle formed by the DPEPO ligand O(1)···Gd(1)···O(2) measures 103.4° in [Gd(1)(hfac)$_3$DPEPO] and O(101)···Gd(101)···O(102) is 89.87° in [Gd(101)(hfac)$_3$DPEPO], both significantly larger than the $H_2O(1)\cdots Gd(1)\cdots O(2)H_2$ angle in $[Gd(hfac)_3(H_2O)_2]$ of 74.3°. Accordingly, the larger steric demands of the DPEPO ligand leads to an average O···Gd···O angle of 70.88° for $[Gd(hfac)_3DPEPO]$ in contrast with 72.28° for $[Gd(hfac)_3(H_2O)_2]$. It is notable, however, that the O(1)···Gd(1)···O(2) and O(101)···Gd(101)···O(102) angles in the two asymmetric units of $[Gd(hfac)_3DPEPO]$ differ by 13.53°. This suggests some flexibility in the arrangement that the DPEPO ligand can adopt within the complex.

Photoluminescence studies of $[Gd(hfac)_3(DPEPO)]$

Photoluminescence properties were studied for a series of Gd complexes, comprising the ligands DPEPO, hfac or both, to identify the singlet and triplet energy levels of the ligands and further our understanding of the origin of the emission in the $[Ln(hfac)_3(DPEPO)]$ series. Gd cannot be excited by energy transfer from the ligands due to the high energy of its first excited state. Therefore, the unquenched luminescence of the ligands can be observed, giving useful information about their excited-state energies.

UV/Vis absorption spectra of the Gd complexes and uncomplexed DPEPO, recorded in DCM solution, are shown in Figure4. The DPEPO shows an absorption onset around 302 nm (33000 cm^{-1}) and λ_{max} = 292 nm (34600 cm^{-1}). $[Gd(hfac)_3(H_2O)_2]$ has a broader absorption than DPEPO shifting the λ_{max} to 298 nm (33500 cm^{-1}, ε = 6400 M^{-1} cm^{-1}) and onset at 345 nm (28900 cm^{-1}). The $[Gd(DPEPO)(NO_3)_3]$ absorption spectrum follows the same shape as the DPEPO ligand but has broader absorption with onset equal to $[Gd(hfac)_3(H_2O)_2]$ (λ_{max} = 292 nm (34500 cm^{-1}, ε = 10200 M^{-1} cm^{-1}). Finally the $[Gd(hfac)_3DPEPO]$ absorption overlaps with all three previous spectra with λ_{max} = 294 nm (33700 cm^{-1}, ε = 20200 M^{-1} cm^{-1}). The onset is the same as the $[Gd(DPEPO)(NO_3)_3]$ and $[Gd(hfac)_3(H_2O)_2]$. The light harvesting of the $[Gd(hfac)_3DPEPO]$ complex with respect to the absorption spectra of the complex $[Gd(hfac)_3(H_2O)_2]$ and DPEPO indicates a synergic effect with enhanced overall absorption in comparison with those of the constituent ligands.

The luminescence spectra of the three Gd complexes are shown in Figure 5. Spectra were recorded in degassed DCM solution at 77 K. The emission originates from the ligand triplet states because the presence of the heavy Gd atom increases the spin-orbit coupling and the rate of intersystem crossing. This effect is shown by the large spectral shift between excitation and emission. Accordingly, the excitation and emission spectra

of [Gd(DPEPO)$(NO_3)_3$] and [Gd(hfac)$_3(H_2O)_2$] reveal the singlet and triplet energy levels of the DPEPO and hfac ligands respectively.

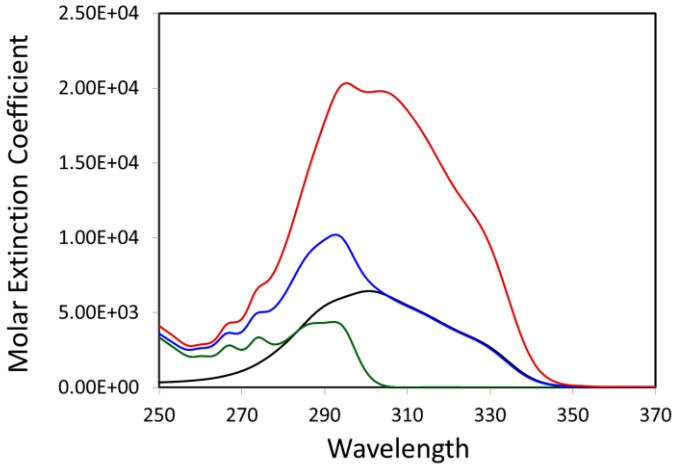

Figure 4. UV/Vis absorption spectra of the DPEPO ligand (green line), Gd(hfac)$_3(H_2O)_2$ (black line), [Gd(DPEPO)$(NO_3)_3$] (blue line), Gd(hfac)$_3$DPEPO (red line).

The lowest triplet energy levels of [Gd(DPEPO)$(NO_3)_3$] and [Gd(hfac)$_3(H_2O)_2$], measured from the high-energy onset of the emission spectra, are found at 27600 cm^{-1} and at 22300 cm^{-1}, respectively. The singlet energy levels, derived from the low-energy onset of the excitation spectra, are at 28900 cm^{-1} for both hfac and DPEPO ligands in the respective complexes.

The emission spectrum of [Gd(hfac)$_3$DPEPO] is almost identical to that of [Gd(hfac)$_3(H_2O)_2$], indicating that the lowest triplet level of the complex is localised on the hfac ligand and there is highly efficient transfer of excitation energy from DPEPO to hfac. The [Gd(hfac)$_3$DPEPO] excitation spectrum looks somewhat distorted and could indicate saturation, but the solutions measured were in the optimal range of absorption ($5x10^{-6}$ M with A = 0.1) and at lower concentration could not be accurately observed. No differences were observed in the emission spectrum while varying the excitation wavelength across the absorption spectrum range. Possible effects of the solid matrix, such as scattering due to aggregation, could account for the unexpected peak shape, however this does not affect the key conclusions regarding the ligand energetics which provide a framework for understanding all the analogous complexes prepared in the series.

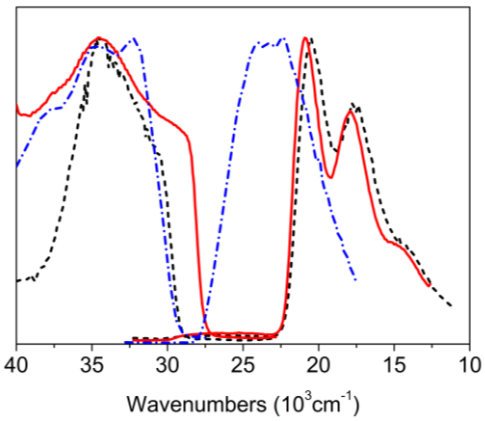

Figure 5. Normalised excitation and emission spectra of $[Gd(hfac)_3(H_2O)_2]$ (black dotted line, λ_{ex} = 310 nm), $[Gd(hfac)_3DPEPO]$ (red solid line, λ_{ex} = 300 nm) and $[Gd(DPEPO)(NO_3)_3]$ (blue dash dot line, λ_{ex} = 315 nm) at 77 K.

Computational Study of $[Eu(hfac)_3(DPEPO)]$

To gain more insight into the nature of the lowest energy triplet state for this family of complexes, a theoretical investigation of $[Eu(hfac)_3(DPEPO)]$ was carried out at the DFT level. The europium complex is of particular interest because of the high quantum yield of around 80%, measured previously.[25] The DFT methodology has been shown in the literature to be a reliable approach to address this type of problem.[33,34] First, geometry optimisation of the $[Eu(hfac)_3(DPEPO)]$ complex in both the lowest-energy singlet and triplet spin states was carried out, without any symmetry constraints (Figure S8†).

Although the crystal structure was obtained for a smaller lanthanide centre (Gd), the optimised structure ground state (Table S2) compares well with the experimental one. In particular, the Ln-O1/Ln-O2 bond lengths are reproduced within 0.05 Å and the Ln-O4/Ln-O5 ones by 0.03 Å (the optimised bond lengths are longer than the experimental ones as expected when using f-in-core RECPs[35]). This agreement clearly demonstrates the ability of the methodology to accurately reproduce the structure of europium complexes.

Analysing the geometry of the triplet state is highly informative regarding the localisation of the ligand excitation. Indeed, in the triplet state, the geometry of the DPEPO ligand remains unchanged whereas one hfac ligand is clearly affected (Table S3). In particular, the C-C bonds of one hfac ligand are elongated by 0.02 Å with respect to the other two. This corresponds to an occupation of the π* orbital of the hfac ligand, indicating that the excitation is primarily located on it. To further confirm this, TDDFT calculations were also carried out from the ground state geometry in order to obtain the vertical excitation. The lowest excitation computed at the TDDFT level corresponds to a singlet-triplet excitation (with three degenerate triplets, one located on each hfac ligand) involving the HOMO and LUMO (and respective LUMO+1 and LUMO+2) orbitals that are located on the hfac ligands (Figure 6). Interestingly, the LUMO is mainly developed on another hfac ligand

(with some residues on the hfac from where the excitation occurs) rather than the one where the HOMO is located. Thus, this triplet state induces population of the π* on one hfac ligand, leading to an increase of the C-C bonds in this ligand. The singlet-triplet gap is computed to be 20950 cm^{-1} which is in excellent agreement with the phosphorescence spectrum of the $[Gd(hfac)_3(H_2O)_2]$ complex, demonstrating that the excitation is located on the hfac ligand. Thus, all the theoretical and experimental analyses point toward localisation of the lowest triplet state on the hfac ligands.

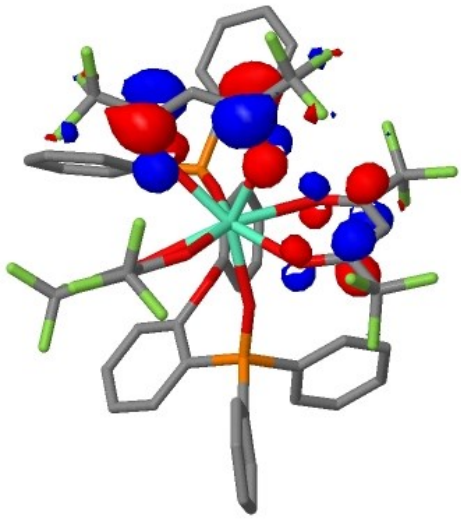

Figure 6. Lowest Unoccupied Molecular Orbital (LUMO) of the $[Eu(hfac)_3(DPEPO)]$ complex populated in the triplet spin state.

Photoluminescence studies of the emissive Ln centres

For the complexes with Ln = Tb, Yb and Nd, absorption, excitation and emission spectra were recorded at room temperature in DCM solutions and these were compared with our previous results for Eu. The absorption and excitation spectra are shown in Figure 7 and 8, respectively and are essentially all superimposable. The consistency of the absorption spectra indicates that the complex absorption is independent of the central lanthanide ion. The consistency between each of the absorption and the corresponding excitation spectra shows that both ligands transfer energy to the metal with equal efficiency since the sensitisation efficiency is independent of wavelength. Although the possibility of direct ligand-singlet-to-Lanthanide energy transfer cannot be excluded,[36,37] the consistency of absorption and excitation spectra across all the Ln ions studied suggests a central role for energy transfer to the lanthanide being funnelled through the lowest triplet state of the hfac ligand in all cases. Narrow emission bands typical of lanthanide complexes were observed (Figure 9), with a shape independent of the excitation wavelength. No emission from free DPEPO[23] was observed, indicating negligible dissociation of the neutral ligand in

solution.[38] The four main emission bands of the Tb^{3+} complex originate from $^5D_4 \rightarrow {}^7F_j$ (with j=6,5,4,3): 20500 cm^{-1}, 18400 cm^{-1}, 17200 cm^{-1}, 16150 cm^{-1}. The Nd^{3+} complex has three narrow emission bands at 11300 cm^{-1} ($^4F_{3/2} \rightarrow {}^4I_{9/2}$), 9410 cm^{-1} ($^4F_{3/2} \rightarrow {}^4I_{11/2}$) and 7485 cm^{-1} ($^4F_{3/2} \rightarrow {}^4I_{13/2}$), and the Yb^{3+} complex has an emission due to the $^2F_{5/2} \rightarrow {}^2F_{7/2}$ transition at 10200 cm^{-1}. From these measurements, energies of the emissive Lanthanide states were determined as follows: Tb = 20500 cm^{-1}, Yb = 10200 cm^{-1}, Nd = 11300 cm^{-1}, Eu = 16300 cm^{-1} (taken from previous work[25]) (Figure 10).

The quantum efficiency of Ln emission, Φ_{Ln}, may be obtained by direct excitation of the lanthanides or estimated by the ratio of the observed and the radiative lifetime τ_{obs}/τ_R, however because τ_R is an estimated value for most lanthanide complexes, this leads only to approximate results for Φ_{Ln}.[10, 39, 40] For many applications, such as light concentration or spectral conversion for solar energy, determination of total photoluminescence quantum yield, Φ_{tot}, is required, and this is the product of the efficiency of ligand sensitisation, η_{sens}, and Φ_{Ln}.

The luminescence decay times, measured in DCM solution at 77 K are given in Table 1. From the ratio of the measured lifetime to the radiative lifetime, the Φ_{Ln} values for the complexes are estimated as: Tb ≤ 50%, Nd ≤ 1%, Yb ≤ 2%, Eu = 78%. The differing values of τ_R reported for Tb[41, 42], Nd[43, 44] and Yb[42, 44, 41] in different recent studies (Table 1) illustrates the uncertainty in the resulting Φ_{Ln} values, hence we report these as upper limits based on the shortest of the above radiative lifetimes in each case. Note that an important exception in this regard is the Eu complex, for which the $^5D_0 \rightarrow {}^7F_1$ magnetic dipole transition is independent of the coordination sphere and can be used as a standard for the dipole strength, allowing τ_R to be accurately determined for any given Eu complex.[45]

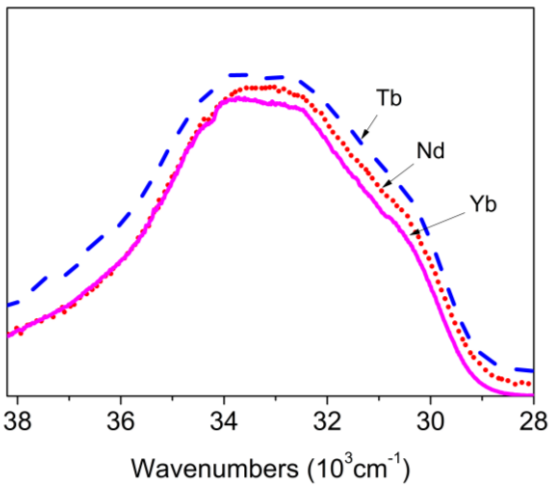

Figure 7. Normalised UV/Vis absorption spectra of the [Ln(hfac)$_3$DPEPO] complexes: Ln = Yb (pink solid line); Ln = Tb (blue dashed line); Ln = Nd (red dotted line); Ln = Gd (black dash dot line). For clarity, the curves are offset along the y-axis.

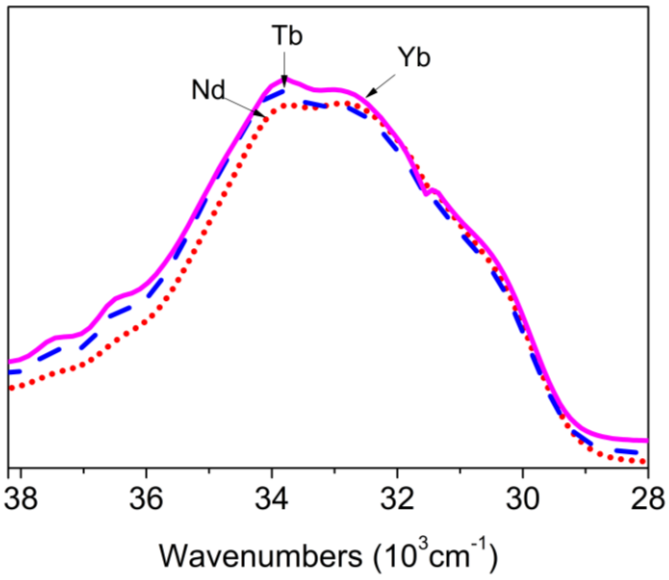

Figure 8. Normalised excitation spectra of the emissive [Ln(hfac)$_3$DPEPO] complexes in DCM at room temperature: Ln = Yb (pink solid line); Ln = Tb (blue dashed line); Ln = Nd (red dotted line). For clarity, the curves are offset along the y-axis. Emission was recorded at the peak emission wavelength of the respective Ln ions.

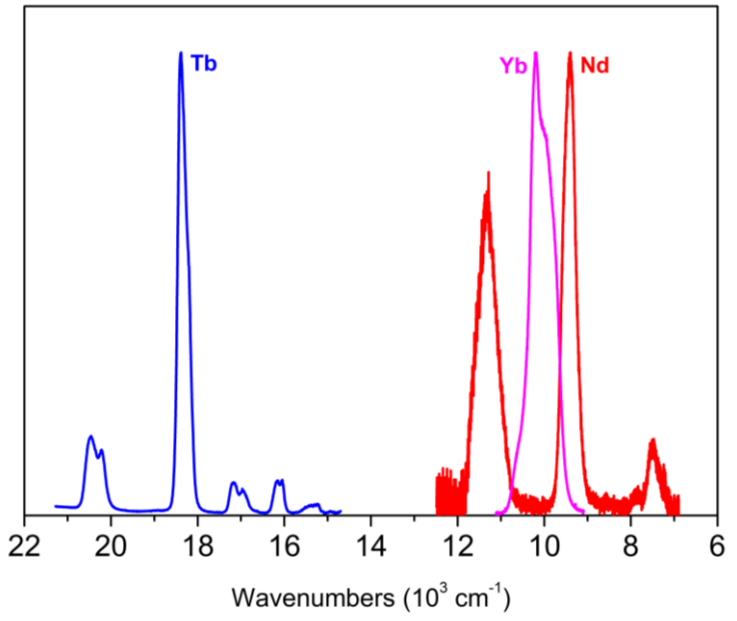

Figure 9. Normalised emission spectra at RT of the compounds: [Ln(hfac)$_3$DPEPO], Ln = Yb (red); Ln = Tb (blue); Ln = Nd (green). The absorbance was 0.1- 0.2 at the excitation wavelength of 295 nm.

Table 1. Observed lifetimes in DCM of [Ln(hfac)$_3$(DPEPO)] compared with literature values of radiative lifetimes.

Ln	τ_R / ms	τ_{obs} / ms)	Φ_{Ln}	PLQY / %
Tb	3.5[41], 1.9[42]	0.95	≤ 50%	6
Nd	0.25[43], 0.613[44]	0.027,	≤ 1%	1
Yb	1.3[42], 1.2[44], 1.2[46]	0.022	≤ 2%	2
Eu	1.11[25]	0.86	78%	76

Lifetime measurements recorded in DCM solution at 77 K. PLQYs are averages of at least four independent measurements with a relative error of 10%, taken with an integrating sphere.

The total photoluminescence quantum yield was determined for Ln = Tb, Yb, Nd and compared with Ln = Eu which we reported previously (Table 1). It is apparent that the complexes Ln = Tb, Yb, Nd each show considerably lower total PLQY than the Eu complex and reasons for this are explored below.

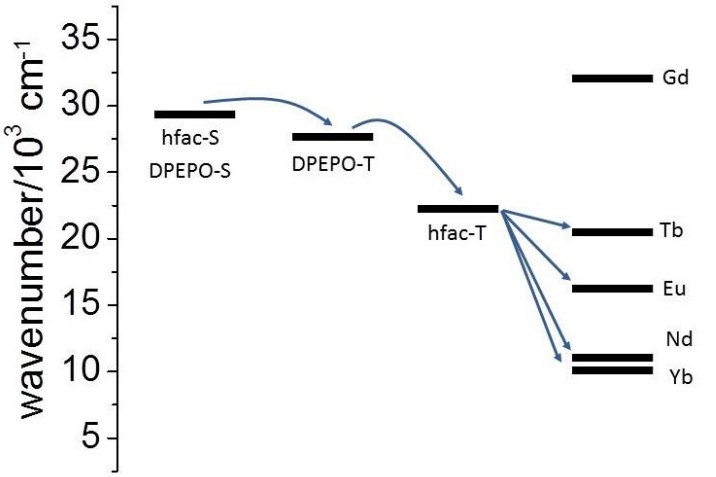

Figure 10. Energy level diagram of [Ln(hfac)$_3$(DPEPO)] showing DPEPO and hfac first excited singlet (left) and triplet (centre) levels alongside the emissive levels of the Ln ions (right). Intersystem crossing and energy transfer pathways are shown.

In the case of Nd and Yb, the emissive energy levels are low (11300 cm^{-1} and 10200 cm^{-1}) and this clearly enables efficient energy transfer from the excited Ln to high-frequency ligand oscillators such as the C-H bonds present in hfac and DPEPO. The much reduced PLQY for these complexes can readily be attributed to this effect, illustrating that the hfac and DPEPO coordination environment, while providing sufficient

protection from high-frequency oscillators to give a high PLQY for Eu, is not sufficiently free of C-H bonds to avoid non-radiative decay in the case of the near-IR emitters Yb and Nd.

Efficient sensitisation of lanthanides requires careful control of the singlet and the triplet excited states. Europium complexes typically have an emissive state around 578 nm (17300 cm^{-1}); the achievement of efficient sensitisation requires the ligand triplet energy level to be at least 2500 cm^{-1} higher (~19800 cm^{-1}) and hence its singlet energy level will be around 24800 cm^{-1}, if it is assumed to be typically around 5000 cm^{-1} higher than the triplet level.[47] Accordingly it is difficult to sensitise Eu efficiently with visible light-absorbing ligands while maintaining very high PLQY, however the singlet energy level of the hfac and DPEPO ligands (around 29000 cm^{-1}) in [Ln(hfac)$_3$(DPEPO)] is significantly higher than this, consistent with the high PLQY when Ln = Eu.

In the case of Tb with a higher-energy emissive state, we would not expect fast vibrational quenching of the Ln emissive state and hence may anticipate a relatively high intrinsic Ln quantum yield. However, the longer radiative lifetime reported for Tb compared with Eu (Table 1) will lead to a significantly lower intrinsic luminescence quantum yield of around 25 – 50%, despite the fact that the observed luminescence lifetime of Tb is comparable with that of Eu. The total PLQY of the Tb complex however is even lower, which we attribute to poor energy transfer from the hfac triplet state to the Tb, due to the higher excited energy level of Tb at 20500 cm^{-1}.

Conclusion

We have prepared a series of lanthanide complexes of formula [Ln(hfac)$_3$DPEPO] and investigated the photophysical properties in the context of structural (Gd) and computational (Eu) results. The resulting comparison has enabled a fuller understanding of the high quantum-yield Eu complex, the role of the hfac and DPEPO ligands and the interaction between them. Some synergic effect between the two ligands was observed in the absorption properties, such that a more intense absorption spectrum of the [Gd(hfac)$_3$DPEPO] complex is shown with respect to the absorption of similar complexes containing each ligand. Furthermore, we have obtained a clear picture of the overall photoluminescence process. Both emission and computational studies agreed that the energy transfer to the Lanthanide ion upon excitation of the molecule comes from the hfac ligand, which has the lower triplet excited state, directly able to transfer its energy to the lanthanide ion. In the case of Tb however, we observe poor energy transfer due to an insufficiently-high triplet energy of the hfac ligand.

Since details of the structure and the energy transfer process are now described, some improvements on the general molecular structure can be addressed. In particular, extending the light harvesting of the Eu complex to longer wavelength is desirable for luminescence downshifting in solar cell applications. An extensively-

conjugated π-electron system could shift the excitation energy to a longer wavelength, possibly without lowering the photoluminescence quantum yield. The DPEPO ligand in particular shows a small gap between the excited singlet and triplet levels and modification of this ligand may lead to better light harvesting while maintaining good energy transfer to Eu provided the triplet DPEPO level remains above that of the hfac. Further work in this direction is underway.

Experimental section

Materials

H_2O, Acetone, Ethanol and Hexane (analytical grade from Acros) were degassed and used without further purification. KO^{t}Bu, 1,1,1,5,5,5-Hexafluoroacetylacetone, $EuCl_3 \cdot 6H_2O$, $TbCl_3 \cdot 6H_2O$, $NdCl_3 \cdot 6H_2O$, $YbCl_3 \cdot 6H_2O$, $GdCl_3 \cdot 6H_2O$ and $Gd(NO_3)_3 \cdot 6H_2O$ were purchased from Sigma-Aldrich. The ligand Bis(2-diphenylphosphino)phenyl) ether oxide was synthesised according to a published procedure.[23]

Synthesis of [Ln(hfac)$_3$(H$_2$O)$_2$] compounds

All the compounds were synthesised according to a procedure analogous to that previously published for the Eu analogue.[25]

Eu(hfac)$_3$(H$_2$O)$_2$ Yield: 46%. ESI MS (MeOH): m/z = 809 $(M\text{-}H)^+$ Found: C, 23.73; H, 0.87. Calc. for $C_{15}H_7EuF_{18}O_8$: C, 22.27; H, 0.87%

Tb(hfac)$_3$(H$_2$O)$_2$ Yield: 52%. ESI MS (MeOH): m/z = 815 $(M\text{-}H)^+$

Found: C, 23.48; H, 0.40. Calc. for $C_{15}H_7F_{18}O_8Tb$: C, 22.08; H, 0.86%

Yb(hfac)$_3$(H$_2$O)$_2$ Yield: 84%. Found: C, 21.64; H, 0.78. Calc. for $C_{15}H_7F_{18}O_8Yb$: C, 21.70; H, 0.85%

Nd(hfac)$_3$(H$_2$O)$_2$ Yield: 53%. ESI MS (MeOH): m/z = 801 (M^+) Found: C, 22.32; H, 0.79. Calc. for $C_{15}H_7F_{18}O_8Nd$: C, 22.48; H, 0.88%

Gd(hfac)$_3$(H$_2$O)$_2$ Yield: 40%. ESI MS (MeOH): m/z = 607 $(M - C_5HF_6O_2)^+$ Found: C, 23.21; H, 0.4. Calc. for $C_{15}H_7F_{18}GdO_8$: C, 22.12; H, 0.87%

Synthesis of [Ln(hfac)$_3$(DPEPO]) compounds

All the compounds were synthesised according to a procedure analogous to that previously published for the

Eu analogue.[25] For the synthesis of [Gd(DPEPO)$(NO_3)_3$] the procedure reported by Xu *et al.* was followed.[23]

[Eu(hfac)$_3$(DPEPO)] Yield: 71%. ESI MS (MeOH): m/z = 1347 (M^-), Found: C, 45.92; H, 1.85. Calc. for $C_{51}H_{31}EuF_{18}O_9P_2$: C, 45.59; H, 2.33%

[Tb(hfac)$_3$(DPEPO)] Yield: 63%. Found: C, 45.24; H, 2.23. Calc. for $C_{51}H_{31}F_{18}O_9P_2Tb$: C, 45.35; H, 2.31%

[Yb(hfac)$_3$(DPEPO)] Yield: 54%. ESI MS (MeOH): m/z = 1159 $(M\text{-}C_5HF_6O_2)^+$, Found: C, 44.71; H, 2.13. Calc. for $C_{51}H_{31}F_{18}O_9P_2Yb$: C, 44.88; H, 2.29%

[Nd(hfac)$_3$(DPEPO)] Yield: 62%. ESI MS (MeOH): m/z = 1128 $(M\text{-}C_5HF_6O_2)^+$, Found: C, 48.03; H, 1.33. Calc. for $C_{51}H_{31}F_{18}NdO_9P_2$: C, 45.85; H, 2.34%

[Gd(hfac)$_3$DPEPO] Yield: 77%. ESI MS (MeOH): m/z = 1142 $(M\text{-}C_5HF_6O_2)^+$, Found: C, 45.38; H, 2.25. Calc. for $C_{51}H_{31}F_{18}GdO_9P_2$: C, 45.41; H, 2.32%

[Gd(DPEPO)$(NO_3)_3$] Yield: 58%. Found: C, 47.60; H, 3.00; N, 4.53. Calc. for $C_{36}H_{28}GdN_3O_{12}P_2$: C, 47.32; H, 3.09; N, 4.60%

Photoluminescence and lifetime measurements

The emission and excitation spectra of [Ln(hfac)$_3$DPEPO)], Ln = Tb, Yb, Nd were measured using an Edinburgh Instruments FS920 spectrometer. Excitation light from a 450 W Xenon lamp was delivered via double monochromators to the sample chamber and emission was detected either by a Peltier cooled R2658P Hamamatsu photomultiplier or a liquid nitrogen cooled Hamamatsu R5509-72 NIR photomultiplier. The photoluminescence quantum yields were determined by absolute measurement using a Horiba Jobin Yvon integrating sphere.[48] All measurements were performed at room temperature in dichloromethane (DCM, spectroscopic grade from Fisher Scientific). Dilute solutions (absorbance 0.1- 0.2 at the excitation wavelength, λ_{exc}) were used for emission measurements. The photoluminescence quantum yields were measured in air-equilibrated solutions. Absorption spectra were obtained by a Varian Cary 50 Scan Spectrophotometer in DCM solution. Excited-state lifetime data in the visible were measured using a Fluoromax-P spectrofluorimeter (Horiba-Jobin-Yvon) in DCM (77 K) and fitted to exponential functions using an iterative non-linear least squares algorithm in the 'Solver' facility in Microsoft Excel. The decay times of NIR emission were measured using a cooled InGaAs detector (Hamamatsu G8605-23), with a time-response of 100 ns FWHM, in combination with an Edinburgh Instruments L900 data acquisition and analysis system. The excitation source was the fourth harmonic (266 nm) of a Q-switched Nd:YAG laser (Continuum Surelite), with pulse width of 10 ns and repetition rate of 10 Hz.

Computational details

Calculations were carried out at the DFT level of theory using the hybrid functional B3PW91.[49,50] Geometry optimisations were carried out without any symmetry restrictions; the nature of the *extrema* (*minima* and transition states) was verified with analytical frequency calculations. All the computations were performed with the Gaussian 03 suite of programs.[51] Europium and Fluorine were represented with a Stuttgart–Dresden pseudo-potential in combination with its adapted basis set.[52,53] The basis set has been augmented by *f* function ($\alpha = 1.0$) for Eu and a set of *d* functions for F.[54] Carbon, nitrogen, oxygen and hydrogen atoms have been described with all electrons 6–31G(*d*,*p*) double–ζ quality basis sets.[55] TDDFT methods were also performed to define the nature of the triplet states.

Crystallographic details

The X-ray crystal structure of [Gd(hfac)$_3$DPEPO] was obtained by slow evaporation from acetone/hexane and determined by single-crystal X-ray crystallography. $C_{51}H_{31}F_{18}GdO_9P_2$, $M = 1348.96$, orthorombic, space group P_{bca}, $a = 24.6540(8)$, $b = 22.2370(7)$, $c = 39.1070(12)$ Å, V = 21439.7 Å^3, $T = 150$ K, $Z = 16$, 327719 measured reflection, 22013 unique ($R_{int} = 0.123$), $R_1 = 0.0471$ ($I > 2\sigma(I)$), w$R_2 = 0.0479$ ($I > 2\sigma(I)$), w$R_2 = 0.0542$ (all data), $\lambda = 0.71073$. Structural images were prepared using the programme Mercury.[56]

Notes and references

[1] M. Elbanowski and B. Ma kowska, *J. Photochem. Photobiol. A*: *Chemistry*, 1996, **99**, 85.

[2] S. V. Eliseeva and J. C. G. Bünzli, *Chem. Soc. Rev.*, **2010**, 189.

[3] S. P. Fricker, *Chem. Soc. Rev.*, 2006, **35**, 524.

[4] B. T. Kilbourn, *Inorg. Chim. Acta*, 1987, **140**, 335.

[5] J. Kido and Y. Okamoto, *Chem. Rev*, 2002, **102**, 2357.

[6] A. de Bettencourt-Dias, *Dalton Trans*, **2007**, 2229.

[7] J. C. G. Bünzli, *Spectroscopic Properties of Rare Earths in Optical Materials*, Springer, 2005, 462-499.

[8] D. B. A. Raj, S. Biju, M. L. P. Reddy, *Dalton Trans*., **2009**, 7519.

[9] J. P. Leonard, T. Gunnlaugsson, *J. Fluorescence*, 2005, **15**, 585.

[10] M. H. V. Werts, R. T. F. Jukes, J. W. Verhoeven, *Phys. Chem. Chem. Phys.*, 2002, **4**, 1542.

[11] L. R. Wilson, B. C. Rowan, N. Robertson, O. Moudam, A. C. Jones, B. S. Richards, *Applied Optics*, 2010, **49**, 1651.

[12] L. Armelao, S. Quici, F. Barigelletti, G. Accorsi, G. Bottaro, M. Cavazzini, E. Tondello, *Coord. Chem. Rev.*, 2009, **254**, 487.

[13] W. H. Weber, J. Lambe, *Applied Optics*, 1976, **15**, 2299.

[14] A. Goetzberger, W. Greube, *Applied Physics A: Materials Science & Processing*, 1977, **14**, 123.

[15] X. Wang, T. Wang, X. Tian, L. Wang, W. Wu, Y. Luo, Q. Zhang, *Solar Energy*, 2011, **85**, 2179.

[16] W. Wu, T. Wang, X. Wang, S. Wu, Y. Luo, X. Tian, Q. Zhang, *Solar Energy*, 2010, **84**, 2140.

[17] K. R. McIntosh, G. Lau, J. N. Cotsell, K. Hanton, D. L. Bätzner, F. Bettiol, B. S. Richards, *Progress in Photovoltaics: Research and Applications*, 2009, **17**, 191.

[18] E. Klampaftis, M. Congiu, N. Robertson, B. S. Richards, *Photovoltaics, IEEE Journal of Photovoltaics*, 2011, **1**, 29.

[19] V. Pawlowski, A. Strasser, A. Vogler, *Z. Naturforsch. B,* 2003, **58**, 950.

[20] S. I. Klink, G. A. Hebbink, L. Grave, A. P. G. B. Oude, F. C. J. M. Van Veggel, M. H. V. Werts, *J. Phys. Chem. A*, 2002, **106**, 3681.

[21] H. Bauer, J. Blanc, D. L. Ross, *J. Am. Chem. Soc.*, 1964, **86**, 5125.

[22] M. Pietraszkiewicz, A. KÅ‚onkowski, K. Staniszewski, J. Karpiuk, S. a. Bianketti, *Journal of Alloys and Compounds*, 2004, **380**, 241.

[23] H. Xu, L. H. Wang, X. H. Zhu, K. Yin, G. Y. Zhong, X. Y. Hou, W. Huang, *J. Phys. Chem. B*, 2006, **110**, 3023.

[24] H. Xu, K. Yin, W. Huang, *Chem. Eur. J.*, 2007, **13**, 10281.

[25] O. Moudam, B. C. Rowan, M. Alamiry, P. Richardson, B. S. Richards, A. C. Jones, N. Robertson, *Chem. Commun.*, **2009**, 6649.

[26] R. D. Hancock, L. J. Bartolotti, *Polyhedron*, 2013, **52**, 284.

[27] R. D. Hancock, *J. Chem. Ed.,* 1992, **69**, 61528.

[28] F. Allen, *Acta Cryst. B*, 2002, **58**, 380.

[29] F. Kennedy, N. M. Shavaleev, T. Koullourou, Z. R. Bell, J. C. Jeffery, S. Faulkner, M. D. Ward, *Dalton Trans.*, **2007**, 1492.

[30] C. Lescop, D. Luneau, P. Rey, G. Bussière, C. Reber, *Inorg. Chem.*, 2002, **41**, 5566.

[31] S. V. Eliseeva, D. N. Pleshkov, K. A. Lyssenko, L. S. Lepnev, J.-C. G. Bünzli, N. P. Kuzmina, *Inorg. Chem.*, 2011, **50**, 5137.

[32] C. R. De Silva, J. R. Maeyer, R. Wang, G. S. Nichol, Z. Zheng, *Inorg. Chim. Acta*, 2007, **360**, 3543.

[33] F. Gutierrez, C. Tedeschi, L. Maron, J.-P. Daudey, R. Poteau, J. Azema, P. Tisnes, C. Picard, *Dalton Trans.*, **2004**, 1334.

[34] F. Gutierrez, C. Tedeschi, L. Maron, J.-P. Daudey, J. Azema, P. Tisnès, C. Picard, R. Poteau, *J. Mol. Struct.*, 2005, **756**, 151.

[35] L. Maron, O. Eisenstein, *J. Phys. Chem. A*, 2000, **104**, 7140.

[36] O. L. Malta, F. R. Goncalves e Silva, *Spectrochim. Acta A*, 1998, **54**, 1593.

[37] C. Yang, L-M. Fu, Y. Wang, J-P. Zhang, W-T. Wong, X-C. Ai, Y-F. Qiao, B-S. Zou, L-L. Gui, *Angew. Chem. Int. Ed.,* 2004, **43**, 5010.

[38] A. Zaim, H. Nozary, L. Guenee, C. Besnard, J-F. Lemonnier, S. Petoud, C. Piguet, *Chem. Eur. J.,* 2012, **18**, 715539.

[39] B. Yan, X. F. Qiao, *J. Phys. Chem. B*, 2007, **111**, 12362.

[40] L. D. Carlos, Y. Messaddeq, H. F. Brito, R. A. S. Ferreira, V. de Zea Bermudez, S. J. L. Ribeiro, *Adv. Mater*., 2000, **12**, 594.

[41] N. Duhamel-Henry, J. L. Adam, B. Jacquier, C. Linarès, *Optical Materials*, 1996, **5**, 197.

[42] A. Aebischer, F. Gumy, J.-C. G. Bünzli, *Phys. Chem. Chem. Phys.*, 2009, **11**, 1346.

[43] S. I. Klink, L. Grave, D. N. Reinhoudt, F. C. J. M. van Veggel, M. H. V. Werts, F. A. J. Geurts, J. W. Hofstraat, *J. Phys. Chem. A*, 2000, **104**, 5457.

[44] M. H. V. Werts, R. T. F. Jukes, J. W. Verhoeven, *Phys. Chem. Chem. Phys.*, 2002, **4**, 1542.

[45] M. J. Weber, T. E. Varitimos, B. H. Matsinger, *Phys. Rev. B*, 1973, **8**, 47.

[46] H. He, A. G. Sykes, P. S. May, G. He, *Dalton Trans.*, **2009**, 7454.

[47] S. Biju, D. B. A. Raj, M. L. P. Reddy, B. M. Kariuki, *Inorg. Chem.*, 2006, **45**, 10651.

[48] L. R. Wilson, B. S. Richards, *Applied Optics*, 2009, **48**, 212.

[49] A. D. Becke, *Chem. Phys*, 1993, **98**, 5648.

[50] K. P. Burke, J. P.; Yang, W., *Electronic Density Functional Theory: Recent Progress and New Directions*, Springer, 1998.

[51] M. J. Frisch, G. W. Trucks, H. B. Schlegel, G. E. Scuseria, M. A. Robb, J. R. Cheeseman, J. J. A. Montgomery, T. Vreven, K. N. Kudin, J. C. Burant, J. M. Millam, S. S. Iyengar, J. Tomasi, V. Barone, B. Mennucci, M. Cossi, G. Scalmani, N. Rega, G. A. Petersson, H. Nakatsuji, M. Hada, M. Ehara, K. Toyota, R. Fukuda, J. Hasegawa, M. Ishida, T. Nakajima, Y. Honda, O. Kitao, H. Nakai, M. Klene, X. Li, J. E. Knox, H. P. Hratchian, J. B. Cross, V. Bakken, C. Adamo, J. Jaramillo, R. Gomperts, R. E. Stratmann, O. Yazyev, A. J. Austin, R. Cammi, C. Pomelli, J. W. Ochterski, P. Y. Ayala, K. Morokuma, G. A. Voth, P. Salvador, J. J. Dannenberg, V. G. Zakrzewski, S. Dapprich, A. D. Daniels, M. C. Strain, O. Farkas, D. K. Malick, A. D. Rabuck, K. Raghavachari, J. B. Foresman, J. V. Ortiz, Q. Cui, A. G. Baboul, S. Clifford, J. Cioslowski, B. B. Stefanov, G. Liu, A. Liashenko, P. Piskorz, I. Komaromi, R. L. Martin, D. J. Fox, T. Keith, M. A. Al-Laham, C. Y. Peng, A. Nanayakkara, M. Challacombe, P. M. W. Gill, B. Johnson, W. Chen, M. W. Wong, C. Gonzalez and J. A. Pople, ed. Gaussian, Wallingford CT, 2004.

[52] M. Dolg, H. Stoll and H. Preuss, *Theoretical Chemistry Accounts: Theory, Computation, and Modeling*, 1993, **85**, 441.

[53] A. Bergner, M. Dolg, W. Kuchle, H. Stoll and H. Preus, *Mol. Phys.*, 1993, **80**, 1431.

[54] L. Maron, C. Teichteil, *Chem. Phys.*, 1998, **237**, 105.

[55] P. C. Hariharan, J. A. Pople, *Theoretical Chemistry Accounts: Theory, Computation, and Modeling*, 1973, **28**, 213.

[56] C. F. Macrae, P. R. Edgington, P. McCabe, E. Pidcock, G. P. Shields, R. Taylor, M. Towler, J. van de Streek, *J. Appl. Crystallogr.* 2006, **39**, 453.